

Configuration Analysis for Power Split Hybrid Vehicles with Multiple Operating Modes

Xiaowu Zhang Chiao-Ting Li Dongsuk Kum Hwei Peng Jing Sun

G041, Lay Auto Lab, 1231 Beal Avenue
Ann Arbor, Michigan, 48109, USA
Phone: (+1-734) 647-9732
Fax: (+1-734) 764-4256
E-mail: xiaowuz@umich.edu

This paper presents a comprehensive analysis for configurations of hybrid electric vehicles with a single planetary gearset and multiple operation modes. The multiple modes are enabled by clutches so that powertrain components can be connected or disconnected from the transmission when necessary. All possible configurations and their possible operating modes are studied systematically. An automatic modeling technique is developed to generate dynamic models for all usable modes in each configuration, so that drivability (acceleration performance) and fuel economy can be analyzed for all configurations. An analytical approach for drivability test is derived to reduce the computation load, and this analytical approach is found to be near-optimal. Fuel economy of all designs is optimized using dynamic programming. Analysis results confirm that the extra flexibility achieved by additional operation modes can improve the vehicle performance.

Topics / Hybrid Electric Vehicle, Power Split Hybrid powertrain, Vehicle design

1. INTRODUCTION

The configuration of hybrid electric vehicles (HEVs) refers to the different ways to connect powertrain components (the engine, electric machines and the output shaft) to the power-split device. For power-split HEVs, the power-split device usually consists of one or multiple planetary gearsets (PGs). The Toyota Prius and the Chevy Volt are two examples of power split HEVs using a single PG. These two vehicles have very different configurations. The Prius uses an input-split configuration (one of the electric machines is connected to the output shaft) with only one operating mode and no clutch, whereas the Volt uses an output-split configuration (one electric machine is connected to the engine) with three clutches and four operating modes. The Prius configuration has been thoroughly studied [1, 2], and there are also analyses on two-PG configurations [3, 4]. Patents of various HEV configuration designs can also be found [5-9].

Despite the fact that there are many patents regarding HEV configuration designs, our previous works have found that the design candidate pool is far larger than what has been studied. For example, for single-PG HEVs, there are 12 different configuration candidates and each of them can have four operation modes [10], and, for two-PG HEVs, there are 1,152 configuration candidates and each of them can have at least two operating modes [11]. In order to identify the best HEV configuration to suit particular vehicle applications, a systematic analysis on all configuration candidate is necessary when given the large candidate pool. This paper focuses on the single-PG configuration

and presents such a systematic analysis for drivability and fuel economy.

In general, a more sophisticated and multi-functional design can lead to better system performance at the cost of structure complexity. This paper demonstrates this idea from two crucial vehicle performance attributes: drivability and fuel economy. For drivability, a fast and near-optimal acceleration test strategy is introduced and applied to verify the basic drivability of the multi-mode hybrid vehicle. For fuel economy study, the dynamic programming (DP) [12-15] will be used to generate the benchmark setter to find the optimal control strategy.

The remainder of this paper is organized as follows: Section 2 explains the dynamics of a single-PG powertrain system and introduces the procedure of configuration search and screening; Section 3 derives an automatic modeling procedure for dynamics of powertrains using a single-PG configuration; Sections 4 and 5 present analyses for drivability and fuel economy; and, Section 6 provides the concluding remarks.

2. CONFIGURATION SEARCH & SCREENING

In this section, the single PG dynamics is first introduced. Systematic configuration search is applied, resulted in 6 input-split and 6 output-split configurations. For each configuration, 8 modes are found initially. After screening procedure, only 4 useful modes are proven to be valid for all 12 configurations.

2.1 Dynamics of a Single Planetary Gearset

A PG consists of a ring gear, a sun gear, a carrier, and several pinion gears, as shown in Fig. 1. A PG can

have two degrees of freedom (DOF), and the rotational speeds of the ring gear, sun gear and the carrier on the PG must follow the relationship shown in Eq. (1)

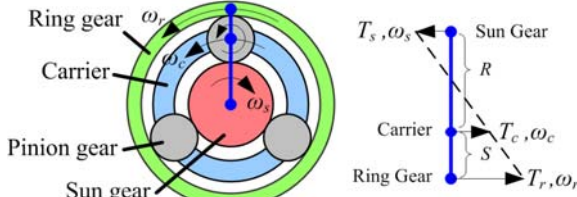


Fig. 1 Planetary Gear [1] and its Lever Analogy

$$\omega_s S + \omega_r R = \omega_c (R + S) \quad (1)$$

During vehicle acceleration, Eq. (1) can be expressed as:

$$\begin{aligned} (\omega_s + \dot{\omega}_s \Delta t)S + (\omega_r + \dot{\omega}_r \Delta t)R \\ = (\omega_c + \dot{\omega}_c \Delta t)(R + S) \end{aligned}$$

Which leads to Eq. (2):

$$\dot{\omega}_s S + \dot{\omega}_r R = \dot{\omega}_c (R + S) \quad (2)$$

Where the subscript *s* denotes the sun gear, *r* denotes the ring gear, and *c* denotes the carrier. *S* and *R* are the radii of the sun gear and ring gear, respectively.

2.2 Configurations of Power-split Powertrains

In this paper, it is assumed that the HEV has one engine and two electric machines (i.e. motor/generator, abbreviated as MGs). Excluding the cases with the engine connecting directly to the output shaft (which is a bad idea), there will be 6 input-split configurations (with one of the two MGs connected to the output shaft) and 6 output-split (with one of the two MGs connected to the engine) [10]. In total, there are 12 potentially useful configurations for power split powertrains using a single-PG.

For all 12 configurations, clutches can be added to disengage powertrain components from the PG or ground a particular PG node to modify the DOF of the PG, leading to different operating modes. Operating modes can be found by adding clutches to all possible locations on the PG. Fig. 2 demonstrates such a concept on an input-split configuration, which is the one used by the Toyota Prius. It is found that 6 clutches can be added to this particular configuration. In fact, it is possible to add one more clutch to separate MG2 and the final drive, so that the output shaft can be disengaged from the powertrain to enable stationary generation, but this possibility will not be discussed in this paper in such case the vehicle is disconnected from the powertrain. This option might be useful for other purposes, but certainly not useful for driving the vehicle.

2.3 Mode Screening

The clutches can be further grouped into three pairs as labeled in Fig. 2, and, with the premises that the two clutches in the same pair must be complementary (i.e. the two clutches cannot be open at the same time), there

are $2^3=8$ possible operating modes, as listed in Fig. 2. Further examination shows that 4 out of the 8 modes are useful. The 4 useful modes are shown in Fig. 3. Note that, in Fig. 3, clutch CL_2 on the engine node is eliminated since 3 clutches (CL_1 , CL_1' , and CL_2') are enough to enable the 4 useful modes.

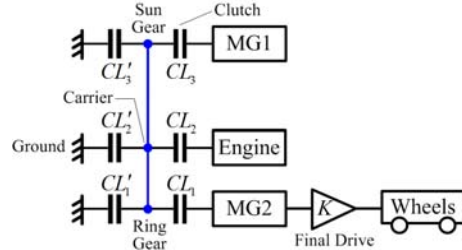


Fig. 2 Possible Clutch Locations for an Input-split Configuration

Table 1 Operation Modes of the Input-split Configuration

Mode	CL ₁	CL ₂	CL ₃
1 (EV ₁)	0	0	1
2 (EV ₂)	1	0	1
3 (Series)	0	1	1
4 (Split)	1	1	1
5 (= EV ₁)	0	0	0
6 (Infeasible)	1	0	0
7 (= EV ₁)	0	1	0
8 (Not EVT*)	1	1	0

Description: “1” means that the clutch is closed; “0” means that the clutch is open. *EVT: Electrically Variable Transmission

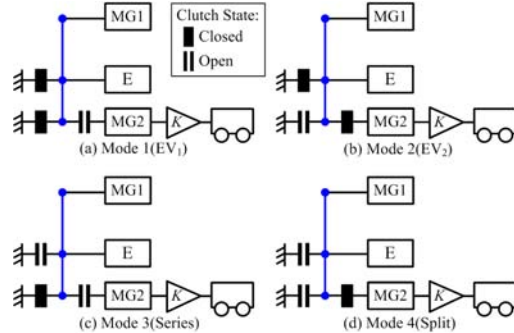


Fig. 3 The Four Useful Operating Modes of Input-split Configurations

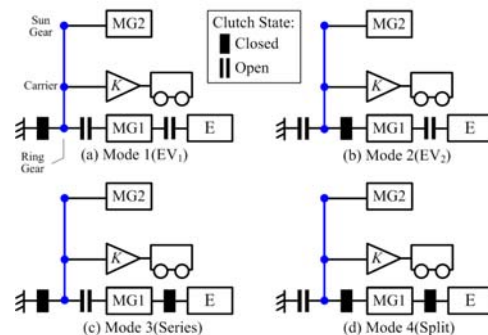


Fig. 4 The Output-split Design—the Chevy Volt

Similar procedures can be applied to output-split configurations to identify useful operating modes. Fig. 4 shows the example configuration search and screening on an output-split configuration, in which 3 clutches are necessary to achieve 4 useful modes. This configuration and 4 modes is actually the design used by the Chevy Volt.

3. MULTI-MODES AUTOMATIC MODELING

In this section, An automatic modeling procedure is proposed based on the dynamic analysis on a single-PG HEV configuration in [10]. The procedure will first derive the dynamic model for the split mode, and then models for the series and electric modes will be obtained by modifying the split mode model. The following presents derivations of the input-split configuration shown in Fig. 3.

Step I: Dynamic model for the split mode is needed for both the input-split and output-split configurations. Eq. (3) and (4) describes the dynamics of the Prius and Volt models which are the typical designs of input- and output-split configuration.

$$\begin{bmatrix} I_e & 0 & 0 & R+S \\ 0 & \frac{mr^2}{K^2} + I_{MG2} & 0 & -R \\ 0 & 0 & I_{MG1} & -S \\ R+S & -R & -S & 0 \end{bmatrix} \begin{bmatrix} \dot{\omega}_e \\ \dot{\omega}_{out} \\ \dot{\omega}_{MG1} \\ F \end{bmatrix} = \begin{bmatrix} T_{MG1} \\ T_{MG2} \\ F \end{bmatrix} \quad (3)$$

$$\begin{bmatrix} I_{MG1} + I_e & 0 & 0 & -R \\ 0 & \frac{mr^2}{K^2} & 0 & R+S \\ 0 & 0 & I_{MG2} & -S \\ -R & R+S & -S & 0 \end{bmatrix} \begin{bmatrix} \dot{\omega}_{MG1} \\ \dot{\omega}_{out} \\ \dot{\omega}_{MG2} \\ F \end{bmatrix} = \begin{bmatrix} T_{MG1} + T_e \\ -T_{Load} \\ T_{MG2} \\ 0 \end{bmatrix} \quad (4)$$

It can be rewritten into a general form

$$A\dot{\Omega} = T \quad (5)$$

where T is the generalized torque vector, $\dot{\Omega}$ is the generalized angular acceleration vector, and A is given by

$$A = \begin{bmatrix} J & D^T \\ D & 0 \end{bmatrix} \quad (6)$$

In the drivability and fuel economy calculations, A need to be inverted to compute the angular accelerations and to eliminate the internal force term F

$$\dot{\Omega} = A^{-1}T \quad (7)$$

The sub-matrix J represents the inertia of the powertrain components whereas the D vector reflects the connections and T_{Load} is the resistance torque measured before the final drive which includes the contributions from the air drag, rolling resistance and braking forces. More generally, it should be noted that Eq. (6) holds for all other configurations. In D vector, its three elements D_1, D_2, D_3 are a permutation of $-R, -S$ and $R+S$: $-R$ means the component is connected to the ring gear node; $-S$ means the component is connected to

sun gear node. $R+S$ means the component is connected to the ring gear node. For the J matrix, each diagonal element corresponds to the inertia of the powertrain component connected to that node, while inertia of the gears is neglected. The T vector contains torque of all components connected to the respective nodes.

Step II: In this step, we will develop models for the other three modes.

Rule 1: When a power device is disconnected and not active, its inertia can be removed from the A matrix.

Rule 2: When the i^{th} node is the only node that is grounded, the i^{th} element of the D and D^T vector is replaced by 0. When the component assigned to the i^{th} node is not active, the $(i,i)^{\text{th}}$ element of the A matrix is replaced by an infinite (in practice, finite but very large) number.

Rule 3: When two nodes of the PG are grounded (the only case is the EV_1 mode of input split configurations), the dynamics is reduced to a trivial equation with the vehicle inertia driven by the motor.

Using the two aforementioned steps, the dynamic models for each configuration can be automatically built for both input-split and output-split configurations.

The generated model will be used in the subsequent drivability verification and the fuel economy discussion, the powertrain parameters and operating ranges are listed in Table 2.

Table 2 Parameters and Operating Range of Powertrain Components

Parameters	MG1	MG2	Engine
Max. Speed (rpm)	12000	12000	4000
Max. Torque (Nm)	200	200	102@4000rpm
Max. Power(kW)	50	50	43
PG Ratio (R:S)	2:1		
Final Drive Ratio	3.95		
Vehicle Mass (kg)	1300		

4. DRIVABILITY ANALYSIS

In this work, the drivability of different HEV configurations is investigated in terms of their acceleration performance. For a traditional vehicle as well as parallel, series HEV and EV, maximum torque from the powertrain components achieve maximum acceleration. For power-split HEV, however, due to the 2 DOF planetary gear, finding the maximum vehicle acceleration is not that straightforward. In other words, maximal torques from all powertrain components do not necessarily correspond to maximum vehicle acceleration. Given the fact we need to search for many vehicle configurations, an efficient way to calculate vehicle maximum acceleration needs to be established.

Fig. 5 demonstrates possible ways to accelerate the vehicle in the split mode, where the accelerations of the output shaft are denoted as $\dot{\omega}_{out}$. We define the ratio between $\dot{\omega}_e$ and $\dot{\omega}_{out}$ as α , shown in Eq. (8).

$$\dot{\omega}_{out} = \alpha \dot{\omega}_e \quad (8)$$

The lever analogy is used to describe the acceleration relationships between each PG node, shown by Eq.(2). The lengths of the arrows reflect the magnitude of angular accelerations. Note that the output accelerations in the ring gear node are the same for (a), (b) and (c).

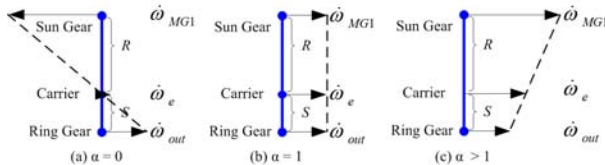


Fig. 5 Different Ways to Accelerate in the Split Mode

In Fig. 5(a), $\alpha = 0$, the engine speed remains constant while the MG1 accelerates in the opposite direction; in Fig. 5(b), all 3 nodes accelerate at the same rate, $\alpha = 1$; in Fig. 5(c), the engine and MG1 accelerate faster than the output shaft, $\alpha > 1$. The number of α should be chosen appropriately so that the instant acceleration of the output shaft should be large enough while speed and torque constrain of MG or engine are less likely to limit the acceleration.

From Eq. (5) and Eq. (8), the required torque from the MG1 and engine with predetermined α and $\dot{\omega}_{out}$ can be calculated from Eq. (9).

$$\begin{bmatrix} T_e \\ T_{MG1} \end{bmatrix} = \begin{bmatrix} K_1 \dot{\omega}_{out} + K_2 (T_{MG2} - T_{Load}) \\ K_3 \dot{\omega}_{out} + K_4 (T_{MG2} - T_{Load}) \end{bmatrix} \quad (9)$$

where,

$$K_1 = \alpha I_e - \frac{D_1}{D_2} I_{FD} \quad (10)$$

$$K_3 = -\left(\alpha \frac{D_1}{D_3} I_{MG1} + \frac{D_2}{D_3} I_{MG1} + \frac{D_3}{D_2} I_{FD} \right) \quad (11)$$

$I_{FD} = mr^2/K^2 + I_{MG2}$ and K_2, K_4 are constant numbers determined by the vehicle parameters. We know that α cannot be excessively large otherwise the torque and speed constraints of the MG and engine will be violated, while since the inertia of the engine and MGs are much smaller than the inertia of the vehicle, the first term of K_1 and K_3 can be neglected. More specifically, using Prius' vehicle parameters,

$$\begin{bmatrix} T_e \\ T_{MG1} \end{bmatrix} = \begin{bmatrix} (0.18\alpha + 10.57)\dot{\omega}_{out} - 25.63(T_{MG2} - T_{Load}) \\ (0.07\alpha - 3.57)\dot{\omega}_{out} + 8.55(T_{MG2} - T_{Load}) \end{bmatrix} \quad (12)$$

It can be seen that if α is within a modest range, its value has little impact on the instantaneous acceleration of the output shaft. That means we can choose α so that all powertrain components accelerate moderately to avoid torque and speed constraints without deteriorating the 0-60 mph acceleration.

In practice, recursive tests can be used to decide the best α number for each vehicle design. However, in practical, we can simply choose $\alpha = 1$ and apply torque calculated from Eq. (9) and get near-optimum result.

Fig. 6 shows a case study for the Prius' input-split configuration with parameters shown in Table 2. And from the result of Dynamic Programming (DP), which is a backward optimization method to get the maximum acceleration performance, we found that the 0-60 mph acceleration results are very similar. This confirms that our simple near-optimal acceleration strategy can quickly assess the vehicle drivability operating in the split mode.

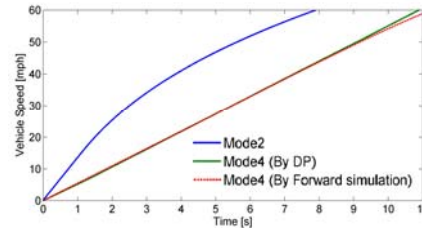


Fig. 6 Comparison of the Speed Trajectories with Vehicle Lurching in Mode2 and Mode4

The two DOF characteristic of PG provides great potential in fuel economy, as demonstrated in the very successful design of Toyota Prius. However, the fact Prius only has one mode (Split mode) also limits its drivability. A grounding clutch on the engine node will moderate this tradeoff. Fig. 6 shows the acceleration performance of Mode 2 (if a ground clutch is added to Prius) compared with Mode 4 (the only mode of Prius). Even without the help from the engine, the vehicle acceleration is far superior. For the other two modes (Mode 1 and Mode 3), the only power source is the 50kW MG2, their acceleration performance is certainly worse than that of Mode 2.

The result in Fig. 6 confirms that the multi-modes design for power split HEV can provide a significant drivability enhancement. NVH (Noise Vibration and Harshness) during mode shift perhaps is a reason why clutches were not used in the Prius design. However, the smooth operation of Chevy Volt shows that the NVH during mode shifts is surmountable. Another possibility is that the small battery in (traditional) Prius limits the launching performance in the EV2 mode, thus adding a clutch does not add much value.

In conclusion, the fast drivability test approach presented in this section can be applied to check the acceleration performance for all configurations operating in the split mode.

5. FUEL ECONOMY ANALYSIS

The Dynamic Programming (DP) technique has emerged as a common tool to find optimal control actions for HEV. This is especially appropriate for vehicle design purposes because it is necessary to judge the merit of a particular configuration based on its performance under the best control execution. The states and control variables used in DP is summarized in Table 3, and the cost function is defined in Eq.(13). Notice that the states of the input-split and the output-split configurations are not identical because of the different ways powertrain components are connected

to the PG. In addition to the mechanical dynamics, the battery SOC is a state variable using the simple internal resistance model to describe battery dynamics.

Table 3. States and Control Variables in DP

DP grid variables	Input-split	Output-split
States	ω_e, SOC	ω_{MG1}, SOC
Control variables	$T_e, T_{MG1}, Mode$	$T_e, T_{MG1}, Mode$

$$\min \left\{ J = \sum_{k=0}^{N-1} (FC_k + \beta \cdot \Delta Mode_k + \gamma \cdot \Delta SOC_k) \right\} \quad (13)$$

The cost function of Eq. (13) consists of three terms: the fuel consumption (FC), penalty on mode shift (FC) and penalty on SOC variation. The mode shift penalty is added to prevent excessive mode shifts while the SOC penalty reflects the fact the battery energy is not free. The SOC penalty will also ensures that the vehicle operates efficiently in EV drive.

In this paper, fuel economy for the Prius configuration (with clutches added) is studied. The same design procedure can be applied to other configurations. The powertrain configurations of the original Prius and the conceptual design Prius⁺⁺ are shown in Fig. 7. The Prius⁺⁺ is obtained by adding three clutches while keeping everything else intact. The original Prius has no clutch and thus only operates in Mode 4, while the Prius⁺⁺ can operate in any of the four modes. The DP solution will choose the best control inputs, including the mode. The optimal fuel consumptions of these two configurations obtained by DP are listed in Table 4. It can be seen that the Prius⁺⁺ achieves a fuel economy improvement of 18% over that of Prius in the urban (FUDS) cycle, which shows the benefit of the additional operation modes.

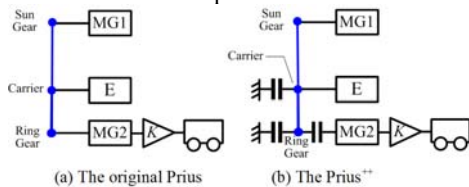


Fig. 7 Schematic Diagrams of the Original Prius and ‘Prius⁺⁺’

Table 4 Optimal Fuel Consumption of Prius/Prius+/Prius++ in the FUDS and HWFET Cycles

Vehicle	Fuel Consumption (g)	
	FUDS	HWFET
Prius (only Mode 4)	117.7	307
Prius ⁺ (Modes 2&4)	96.2	302
Prius ⁺⁺ (all four modes)	95.7	302

Further analysis on the DP solutions shows that the Prius⁺⁺ mainly operates in Modes 2 and 4 (see Fig. 8). The other two modes are rarely used. Therefore, we looked into an alternative design, the Prius⁺, which has only one clutch to switch between Mode 2 and Mode 4. The Prius⁺ configuration is shown in Fig. 9. The fuel economy of Prius⁺ is also listed in Table 4, and its DP

solution is shown in Fig. 10. Comparing Fig. 8 and Fig. 10, we can see that the optimal mode selection of the Prius⁺ is very close to that of the Prius⁺⁺, and the fuel economy is also similar. This indicates that the one-clutch design can achieve near-optimal fuel economy (compared with the three-clutch design).

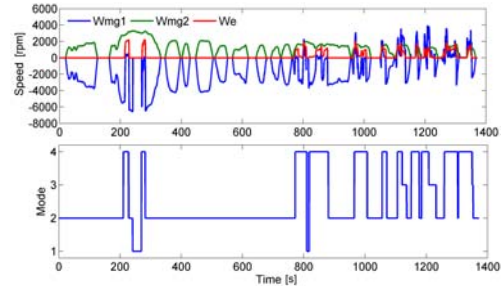


Fig. 8 The Speeds and Mode Selection of Prius⁺⁺ in the FUDS Cycle.

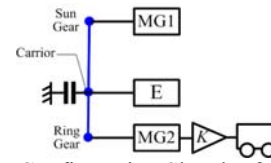


Fig. 9 The Configuration Sketch of the ‘Prius⁺’.

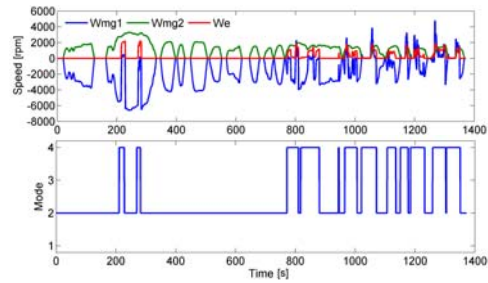


Fig. 10 The Speeds and Mode Selection of Prius⁺ in the FUDS Cycle.

The highway driving fuel economy is also examined for all the three variations (Prius, Prius⁺ and Prius⁺⁺) using the HWFET cycle. The optimal fuel consumptions are very close (see Table 4), which means the benefit of additional modes in highway driving is minimal.

We applied the same design procedure to analyze the output split configuration used by Volt, and found that 2 clutches can be removed with almost no impact on drivability and fuel economy, as shown in Table 5. The simplified powertrain designed is termed ‘Volt⁻’, as shown in Fig. 11.

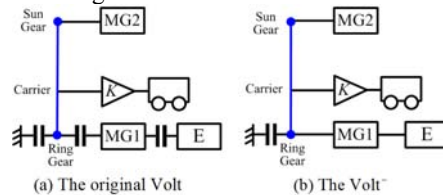


Fig. 11 The Original Volt and the Volt⁻

Table 5 Fuel Consumption and Acceleration Performance of Volt and the Proposed Volt⁺ Design

Vehicle	Fuel Consumption		0~60 mph acceleration (sec)
	FUDS	HWFET	
Volt (All 4 Modes)	125.8	320.5	8.5
Volt ⁺ (Modes 1&4)	125.8	323.2	8.8

In summary, adding a single clutch to the carrier gear (Fig. 9) to add "Mode 2" to the Prius configuration is beneficial for both drivability and fuel economy in urban driving. In addition, it was found that reducing 2 clutches from the original Volt design results in almost identical drivability and fuel economy performance.

6. CONCLUSION

A previous work [10] presents a thorough analysis of all possible configurations of power-split hybrid powertrain using a single PG. It was found that adding 3 clutches enables 4 useful modes (EV1, EV2, series and split modes) in all the input-split and output-split HEVs.

In this paper, an automatic modeling procedure is developed to obtain the dynamic models for all 12 configurations with 4 modes. Drivability analysis indicates that the split mode, despite of the fact all three power sources are connected, may have lower acceleration (compared with EV modes) due to the 2 degree of freedom nature of the powertrain. A fast way to compute vehicle acceleration performance is established for split mode and its near-optimality is proven by comparing with DP solutions. In addition, it is shown that the introduction of additional modes by adding clutches can render a much better drivability to the vehicle. More specifically, for the input-split configuration used in the Toyota Prius, if a grounding clutch is added to the engine (carrier gear) node, resulting in the so-called Prius⁺, the 0-60 time is reduced by 24%. We further analyzed the fuel economy of the powertrain configuration used by the Toyota Prius. The Prius⁺, with one clutch and two modes (Modes 2&4), achieves fuel economy 18% better than the original Prius in the FUDS cycle. However, adding modes has little fuel economy benefits for the HWFET cycle. While for Volt, removing 2 clutches has almost no impact to vehicle fuel economy and launching performance. This design and analysis procedure can be applied to other single planetary gear designs and will be extended to analyze power-split designs using two planetary gearsets.

7. AKNOWLEDGEMENT

This material is based upon work supported by the Department of Energy under Award Number DE-PI0000012.

8. REFERENCES

- [1] J. Liu and H. Peng, "Modeling and control of a power-split hybrid vehicle," *IEEE Transactions on*

Control Systems Technology, vol. 16, pp. 1242-1251, 2008.

- [2] C. Mansour and D. Clodic, "Dynamic modeling of the electro-mechanical configuration of the Toyota Hybrid System series/parallel power train," *International Journal of Automotive Technology*, vol. 13, pp. 143-166, 2012.
- [3] B. Conlon, "Comparative analysis of single and combined hybrid electrically variable transmission operating modes," *SAE Paper*, 2005-01-1162, 2005.
- [4] T. Grewe, B. Conlon, and A. Holmes, "Defining the general motors 2-mode hybrid transmission," *SAE Paper*, 2007-01-0273, 2007.
- [5] M. Schmidt, "Two-mode, compound-split electro-mechanical vehicular transmission," *U.S. Patent 5 931 757*, 1999.
- [6] M. Schmidt, "Two-mode, input-split, parallel, hybrid transmission," *U.S. Patent 5 558 588*, 1996.
- [7] A. Holmes, D. Klemen, and M. Schmidt, "Electrically variable transmission with selective input split, compound split, neutral and reverse modes," *U.S. Patent 6 527 658 B2*, 2003.
- [8] X. Ai and S. Anderson, "Two-mode, compound-split, vehicular transmission having both enhanced speed tractive power," *U.S. Patent 2006/0111212 A9*, 2000.
- [9] M. Raghavan, N. Bucknor, and J. Hendrickson, "Electrically variable transmission having three interconnected planetary gear sets, two clutches and two brakes," *U.S. Patent 7 179 187*, 2007.
- [10] X. Zhang, C.-T. Li, D. Kum, and H. Peng, "Prius+ and Volt-: Configuration Analysis of Power-Split Hybrid Vehicles with a Single Planetary Gear," *IEEE Transactions on Vehicular Technology*, under review.
- [11] J. Liu and H. Peng, "A systematic design approach for two planetary gear split hybrid vehicles," *Vehicle System Dynamics*, vol. 48, pp. 1395-1412, 2010.
- [12] A. Brahma, Y. Guezennec and G. Rizzoni, "Optimal energy management in series hybrid electric vehicles", *American Control Conference*, vol.1, pp. 60-64, 2000.
- [13] C.-C. Lin, H. Peng, J. Grizzle, and J.-M. Kang, "Power management strategy for a parallel hybrid electric truck," *IEEE Transactions on Control Systems Technology*, vol. 11, pp. 839-849, 2003.
- [14] J. Liu and H. Peng, "Control optimization for a power-split hybrid vehicle," in *American Control Conference*, Minneapolis, Minnesota, 2006, pp. 466-471.
- [15] S.J. Moura, H.K. Fathy, D.S. Callaway, J.L. Stein, "A stochastic optimal control approach for power management in plug-in hybrid electric vehicles", *IEEE Transactions on Control System Technology*, vol. 19, pp. 545-555, 2011